Sequential memory: Binding dynamics

Cite as: Chaos **25**, 103118 (2015); https://doi.org/10.1063/1.4932563
Submitted: 22 July 2015 . Accepted: 22 September 2015 . Published Online: 13 October 2015

Valentin Afraimovich, Xue Gong, and Mikhail Rabinovich

Sequential memory: Binding dynamics

Valentin Afraimovich,[1] Xue Gong,[2,a)] and Mikhail Rabinovich[3]
[1]*IICO-UASLP, Karakorum 1470, Lomas 4a, San Luis Potosi, SLP 78210, Mexico*
[2]*Department of Mathematics, Ohio University, Athens, Ohio 45701, USA*
[3]*BioCircuits Institute, University of California San Diego, 9500 Gilman Dr., La Jolla, California 92093-0328, USA*

(Received 22 July 2015; accepted 22 September 2015; published online 13 October 2015)

Temporal order memories are critical for everyday animal and human functioning. Experiments and our own experience show that the binding or association of various features of an event together and the maintaining of multimodality events in sequential order are the key components of any sequential memories—episodic, semantic, working, etc. We study a robustness of binding sequential dynamics based on our previously introduced model in the form of generalized Lotka-Volterra equations. In the phase space of the model, there exists a multi-dimensional binding heteroclinic network consisting of saddle equilibrium points and heteroclinic trajectories joining them. We prove here the robustness of the binding sequential dynamics, i.e., the feasibility phenomenon for coupled heteroclinic networks: for each collection of successive heteroclinic trajectories inside the unified networks, there is an open set of initial points such that the trajectory going through each of them follows the prescribed collection staying in a small neighborhood of it. We show also that the symbolic complexity function of the system restricted to this neighborhood is a polynomial of degree $L - 1$, where L is the number of modalities. © *2015 AIP Publishing LLC*.
[http://dx.doi.org/10.1063/1.4932563]

Human mental functions like perception, cognition, and social interaction depend upon coordinated brain network activity. Such a coordination operates within noisy, overlapping modes of these networks on different levels of a cognitive hierarchy. Usually, the performance of cognitive task, for example, memory recall or generation of ideas, is a sequential dynamical process of switching among different information items or cognitive modes in a winnerless competitive manner. In fact, while we are thinking about a sequence of episodes or complex objects, the mind unifies several representing operations with different features of such episodes or objects. This is a binding process. For successful performance, the binding dynamics has to be stable or robust against noise. Mathematical aspects of this problem are considered in this paper.

I. INTRODUCTION

There are several types of sequential memory (SM), which can be divided into the kinds of memory that are expressed explicitly, that is, by direct conscious access to information (declarative memory), and the kinds of memory that are expressed implicitly through changes in behavioral or physiological responses in the absence of conscious access (non-declarative memory). One particular form of declarative memory is episodic memory—the ability to encode and retrieve the sequence of events in our daily personal activities. Such memory is supported by cooperation of many cortical and subcortical structures.[1] Another type of sequential memory is working memory that is involved in the short-term maintenance of information in mind, and the manipulation of this information for the purpose of achieving an immediate goal. The simplest example is remembering a phone number while picking up and dialing a phone. Working memory is also important for comprehending long written or spoken sentences, performing and holding in mind a string of new information or a series of movements. Declarative memories typically include information about time and place of an event, as well as detailed information about the event itself.

SM dealing with sequential order of thoughts or events provides the functional backbone to high-level cognition. Maintenance in SM is assumed to depend on the persistence of functional networks that represent memory information content. Imaging methods for measuring and analyzing population-level brain patterns show that activity of memory networks is highly dynamic.[2] Corresponding to the performance of the SM, brain dynamics involves different partially overlapping brain functional networks. Their interconnections change in time according to the performance stage, and can be stimulus-driven or induced by an intrinsically generated goal. Such brain activity can be described by spatiotemporal discrete patterns or sequentially changing dynamical modes.

At first glance, such a dynamics seems at odds with the very nature of keeping information items in SM. How can we recall a stable order of thoughts, episodes, etc., in mind while the brain activity is constantly changing? The answer to this question can be very useful for the understanding of different mental disorders and for the role of emotions in sequential memory binding.[3]

This paper is based on models that authors have developed before. In the paper Ref. 4 in 2001 and after this in Ref. 5, it was suggested a new paradigm for neurocognitive science—dynamical encoding of environmental or

a)Electronic mail: xg345709@ohio.edu

memory information on the base of networks with sequential competition. This paradigm is called Winnerless Competition (WLC) principle. The key point of this paradigm is a transformation of a simple even static incoming information into spatio-temporal patterns which is very convenient for recognition (decoding) through a competitive dynamical process. What is important is that the temporal dynamics of such patterns can be not repetitive. According to this, we introduced in 2004 "the robust heteroclinic transient," which became now an important tool for the analyses of speech and behavioral sequences.[6] It is very convenient for the investigation of SM on its stability and capacity.

II. LOW-DIMENSIONAL DYNAMICAL MODEL OF SM: HETEROCLINIC BINDING

Nonlinear dynamical modeling of human SM dynamics can be considered as a functionally oriented variant of a universal scale free cognitive model. Such canonical model of cognitive dynamical processes has been introduced in Ref. 7. This model is based on the following principles: (i) equations are written with variables that can represent the evolution of brain elements in their temporal coherency and have solutions that correspond to metastable patterns in the brain; (ii) the model is based on the winnerless competitive dynamics—a nonlinear process of interaction of many agents that guarantees sequential switching among metastable states and robustness of transients;[4,5] (iii) the model is an open dissipative system where inhibition is balanced by excitation; and (iv) the model's dynamics is sensitive to the incoming information.

By definition, WLC in simple network ($N=3$) leads to a heteroclinic cycle, but the same network with other values of parameters can have limit cycles, for example, in a vicinity of the unstable focus in the middle of the simplex. Such limit cycle does not represent sequential switching of competitors activity, it reflects just small oscillation of their intensity. In systems with $N>3$, WLC leads to robust heteroclinic transient (see Appendix B).

The reduction of high-dimensional brain data to a low-dimensional phase space is a very attractive idea that can be motivated by empirical observation. In particular, there are many experiments that have shown the low-dimensionality of cognitive dynamics when it is governed by sensory stimuli. Formally, this means that a large amounts of data can be extracted from the dynamics of a reduced number of spatiotemporal patterns—modes—using spatiotemporal decomposition techniques, such as principal component analysis[8–10] and independent component analysis.[11,12] For a review, see Ref. 13.

Adopted to the binding sequential processes, a model has been proposed in Ref. 14. This model (1), in fact, is a canonical Gause-Lotka-Volterra model, which is written in a specific form that is convenient for the analyses of the structured competitive dynamics, specifically for the binding (see also Appendix B)

$$\frac{dx_i^l}{dt} = x_i^l\left(\sigma_i^l - \sum_{j=1}^{N}\rho_{ij}^l x_j^l - \sum_{m=1}^{L}\sum_{j=1}^{N}\xi_{ij}^{lm}x_j^m\right)$$
$$\text{for } i=1,\ldots,N; l=1,\ldots,L, \qquad (1)$$

where x_i^l is the level of activity of the i-th mode in the l-th informational modality, where $i=1,\ldots,N$, and $l=1,\ldots,L$. Information mode variables x_i^l must be nonnegative for all i, l. Integer NL is the total number of modes describing the components from different brain areas that interact to perform a sequential memory process. Time constants are fixed for a given system. Parameters ρ_{ij}^l describe the inhibitory connections between modes i and j in the l-th modality, while parameters ξ_{ij}^{lm} describe such connections between modes i in the l-th modality and j in the m-th modality. We assume $\rho_{ii}^l=1$ and $\xi_{ii}^{ll}=0$ for any i and l. Parameters σ_i^l are the strength of the stimulation of the mode i in the l-th modality. It is important that, in general, the entries of the matrix consisting of parameters ξ_{ij}^{lm} control the binding process.

We are talking about memory, i.e., a cognitive function. Let us define a cognitive mode as a temporary stable activity pattern of correlated elements in a specific global brain network. Because of the high level of intrinsic coherency, the dynamics of complex cognitive modes can be described just with a small number of variables in a model. This number depends on the hierarchical structure of the cognitive process. Elements of sequential memory also are named as information memory items. In particular, they can be digits that form a phone number (about stability of such sequences see Ref. 7). Information item memory concerns the processing, storage, and retrieval of specific information, such as a word, color, smell, or a recognizable shape of the car. The combining into one unified block of items of different natures from different modalities or different sources—like color, taste, odor, and after tasting in the wine degustation—named binding process. Sequential changing of the item blocks characterizes the information flow.

For $L=3$, an architecture of coordinated functional ensembles each of which sequentially represents specific modality is depicted in Fig. 1. In fact, the model (1) is a canonical Gause-Lokta-Volterra model written in the form that is convenient for the analyses of the binding phenomena, see Subsection 1 in Appendix B.

As computer experiment showed, the dynamics of three-modality SM is very rich and sensitive to the incoming information that controls system parameters. At the same time, such dynamics is robust and reproducible. We found different robust regimes in the framework of the model (1), in particular, heteroclinic cycles and binding regime. One of the robust binding regimes is presented in Figs. 2 and 3 (see also Ref. 14).

It is important to mention robust heteroclinic cycles and, in general, robust transients consisting of trajectories in the phase space of a dynamical model that are disposed in a vicinity of a heteroclinic contour or a heteroclinic chain and in a vicinity of each other when initial conditions are varied. These trajectories are robust against noise. Examples of such transients are the trajectories inside the stable heteroclinic channel (SHC).

This modeling showed that the information flows corresponding to different modalities modulate each other and as a result, the dynamical behavior of individual modality contains information about all other modalities (see Figs. 2 and 3). This is an information binding. In fact, Figs. 2 and 3 illustrate a multimodal concurrency—the main mechanism of multimodal serial order in behavior.[35]

III. ROBUSTNESS THEOREM

We can find the equilibrium points of the system $Q_i^l = \{x_i^l = \sigma_i^l, x_j^m = 0 \text{ if } j \neq i, m \neq l\}$. For each Q_i^l where $i = 1, \ldots, N$ and $l = 1, \ldots, L$, the eigenvalues and eigenvectors are given in Table I.

In Ref. 14, the authors assumed that starting at each Q_i^l, there are two heteroclinic orbits, toward Q_{i+1}^l and Q_i^{l+1}. Therefore, at each equilibrium point, only two eigenvalues corresponding to these two directions are positive and the rest of the eigenvalues are negative. We can list the assumptions as follows. (Note that only λ_{ii+1}^l and λ_{iN+1}^l are positive for fixed i and l, the other eigenvalues are negative.)

For fixed $l = 1,2,\ldots,L$, within the l-th modality:

1. $\lambda_{ii+1}^l = \sigma_{i+1}^l - \sigma_i^l(\rho_{i+1i}^l + \xi_{i+1i}^{ll}) > 0$ and $\lambda_{ij}^l = \sigma_j^l - \sigma_i^l(\rho_{ji}^l + \xi_{ji}^{ll}) < 0$ for all $j \neq i, i+1$ so that there is only one heteroclinic orbit from Q_i^l to Q_{i+1}^l.
2. $\max_{1 \leq j \leq N, j \neq i+1}\{\lambda_{ij}^l\} = \lambda_{ii-1}^l < 0$ for each $i = 1,\ldots,N$, $(N+1 \equiv 1)$. We assume that the heteroclinic trajectory joining the saddles Q_{i-1}^l and Q_i^l follows the leading direction on the stable manifold of Q_i^l. The point Q_i^{l+1} is a stable node on the (x_i^l, x_i^{l+1})-plane.
3. The saddle value of Q_i^l is $\nu_i^l := [\sigma_{i-1}^l - \sigma_i^l(\xi_{i-1i}^{ll} + \rho_{i-1i}^l)] / [\sigma_{i+1}^l - \sigma_i^l(\rho_{i+1i}^l + \xi_{i+1i}^{ll})] > 1$ and $\nu^l = \Pi_{i=1}^N \nu_i^l > 1$.

It was shown in Ref. 14 that under the conditions 1–3, the system (1) has a stable heteroclinic cycle Γ_l in the invariant subspace $\{x_j^m = 0, m \neq l\}$.

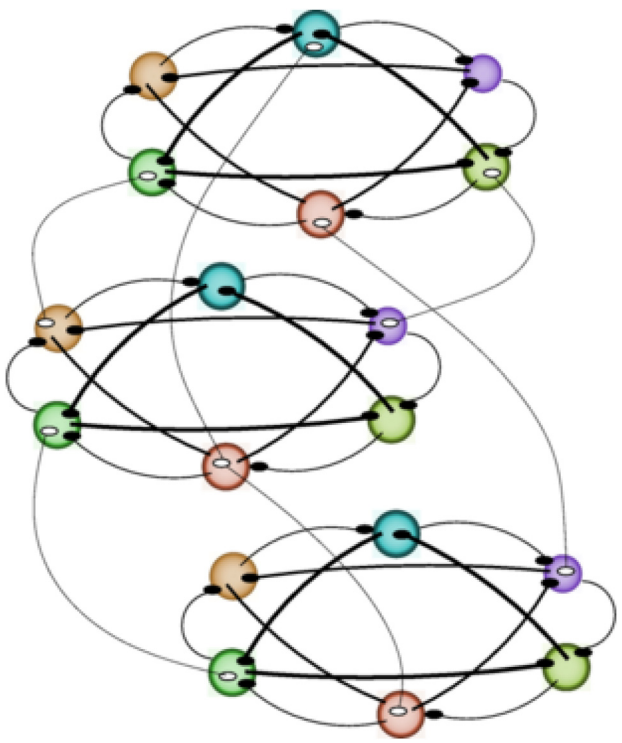

FIG. 1. Eighteen competitors ensemble fluctuates on three functional communities: each of them is responsible for the processing of different informational modalities. All connections are inhibitory. The connections in corresponding models are characterized by entries in matrices of ρ_{ij}^l and ξ_{ij}^{lm}. Reprinted with permission from M. I. Rabinovich, A. N. Simmons, and P. Varona, "Dynamical bridge between brain and mind," Trends Cognit. Sci. **19**, 453–461 (2015). Copyright 2015 Elsevier.

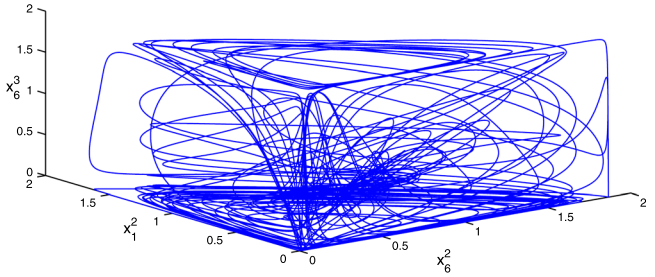

FIG. 2. Binding: mutual modulations of different modalities sequences. These figure show the projection of a trajectory on a three-variable space. One can see that the trajectory spends some time in a neighborhood of one modality and goes to the next modality afterwards.

For fixed $i = 1, 2,\ldots, N$, consider the equilibrium points Q_i^l corresponding to different modalities l:

4. $\lambda_{iN+l+1}^l = \sigma_i^{l+1} - \sigma_i^l \xi_{ii}^{zl+1l} > 0$ for every $l = 1, 2,\ldots,L-1$ so that there is a heteroclinic orbit from Q_i^l to Q_i^{l+1}.
5. $0 < \lambda_{iN+l+1}^l < \lambda_{ii+1}^l$, i.e., $0 < \sigma_i^{l+1} - \sigma_i^l \xi_{ii}^{zl+1l} < \sigma_{i+1}^l - \sigma_i^l(\xi_{i+1i}^{ll} + \rho_{i+1i}^l)$. We assume here the unstable leading direction within the modality is stronger than that between modalities, so that the representative point on a trajectory spends a large amount of time around a modality subspace before going to another subspace.

Denote by Γ the heteroclinic network consisting of heteroclinic cycles Γ_l and heteroclinic trajectories joining them. It was shown in Ref. 14 that such a heteroclinic network exists under the assumptions 1–5. Identify with Γ the directed graph G see Fig. 4, with vertices Q_i^l such that there is an edge starting at Q_i^l and ending at Q_j^m if and only if there is a heteroclinic trajectory going to Q_i^l as $t \to -\infty$ and to Q_j^m as $t \to +\infty$. Let us enumerate vertices by numbers 1, 2, …, p, where $p = LN$. Introduce a matrix $A = \{a_{sk}\}$, $a_{sk} \in \{0, 1\}$, where $a_{sk} = 1$ iff there exists an edge starting at the s-vertex and ending at the k-vertex. We introduce the topological Markov Chain (Ω_A, σ) associated with the transition matrix A. Any non-empty cylinder $[\omega_0, \omega_1, \ldots, \omega_k]$ corresponds to a path on the graph G, i.e., a sequence of the saddle equilibrium points and heteroclinic trajectories joining them belonging to Γ. For $[\omega_0, \omega_1, \ldots, \omega_m]$,

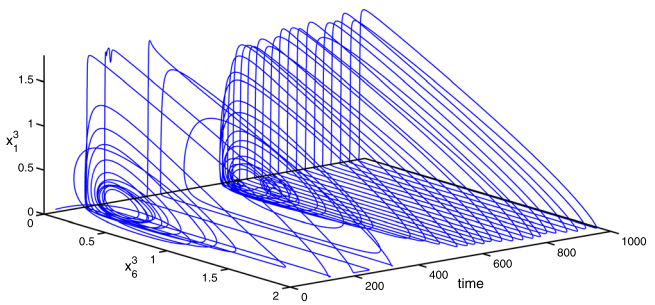

FIG. 3. This figure shows the sequential switching among modes of one modality in the binding process. Parameters used in model (1) for both Figs. 2 and 3 are $L = 3$, $N = 6$, $\sigma_1^l = 1.73, \sigma_2^l = 1.123, \sigma_3^l = 1.301, \sigma_4^l = 1.203, \sigma_5^l = 1.458$, and $\sigma_6^l = 1.903$ for all $l = 1, 2, 3$; $\rho_{ii}^1 = 1$ for $i = 1, \ldots, 6$, $\rho_{13}^1 = \rho_{35}^1 = \rho_{51}^1 = 5$, $\rho_{24}^1 = \rho_{46}^1 = \rho_{64}^1 = 2$, $\rho_{16}^1 = \rho_{21}^1 = \rho_{32}^1 = \rho_{43}^1 = \rho_{54}^1 = \rho_{65}^1 = 1.5$ and the rest of ρ_{ij}^1 is 0. We allow a 2% perturbation on parameter values ρ_{ij}^l in the other two modalities, i.e., $\rho_{ij}^2 = \rho_{ij}^1 + 2\%$ and $\rho_{ij}^3 = \rho_{ij}^1 - 2\%$ if $\rho_{ij}^1 \neq 0$; for the connection between the modalities, we let $\xi_{ij}^{lm} = 0.1$ if i and j are both odd integers and $l \neq m$ and all the other values for ξ_{ij}^{lm} are 0.

TABLE I. Eigenvalues and eigenvectors at the equilibrium point Q_i^l.

Eigenvalues	Eigenvectors
$\lambda_{ij}^l = \sigma_j^l - \sigma_i^l(\xi_{ji}^{ll} + \rho_{ji}^l)(1 \le j \le N, j \ne i, i+1)$	$\vec{v}_{ij}^{\,l} = \{x_i^l = \xi_{ij}^{ll} + \rho_{ij}^l, x_j^l = \xi_{ji}^{ll} + \rho_{ji}^l - 1 - \sigma_j^l/\sigma_i^l, \text{others} = 0\}$
$\lambda_{ii}^l = -\sigma_i^l$	$\vec{v}_{ii}^{\,l} = \{x_i^l = 1, \text{others} = 0\}$
$\lambda_{ii+1}^l = \sigma_{i+1}^l - \sigma_i^l(\xi_{i+1i}^{ll} + \rho_{i+1i}^l)$	$\vec{v}_{ii+1}^{\,l} = \{x_i^l = \xi_{ii+1}^{ll} + \rho_{ii+1}^l, x_{i+1}^l = \xi_{i+1i}^{ll} + \rho_{i+1i}^l - 1 - \sigma_{i+1}^l/\sigma_i^l, \text{others} = 0\}$
$\lambda_{iN+l+1}^l = \sigma_i^{l+1} - \sigma_i^l \xi_{ii}^{l+1l}$	$\vec{v}_{iN+l+1}^{\,l} = \{x_i^l = \xi_{ii}^{ll+1}, x_i^{l+1} = \xi_{ii}^{l+1l} - 1 - \sigma_i^{l+1}/\sigma_i^{l+1}, \text{others} = 0\}$
$\lambda_{iN+m}^l = \sigma_i^m - \sigma_i^l \xi_{ii}^{ml} (1 \le m \le L, m \ne l, l+1)$	$\vec{v}_{iN+m}^{\,l} = \{x_i^l = \xi_{ii}^{lm}, x_i^m = \xi_{ii}^{ml} - 1 - \sigma_i^m/\sigma_i^m, \text{others} = 0\}$

the trajectory starts at the ω_0-th vertex, follows a heteroclinic orbit to the ω_1-th vertex, then follows another heteroclinic orbits to the ω_2-th vertex, and so on until it reaches the ω_m-th vertex. Denote this subnetwork by $\Gamma([\omega_0, \omega_1, \ldots, \omega_k])$ and call it a *multimodality heteroclinic network* (MHN). Without loss of generality, we may assume that ω_0 is a symbol that is labeling a saddle $Q_1^l \in \Gamma_1$, a vertex of the graph. We will define $P_{l_m}^m$ as the heteroclinic trajectory in $\Gamma([\omega_0, \omega_1, \ldots, \omega_k])$ joining the saddles $Q_{l_m}^m$ and $Q_{l_m}^{m+1}$.

The feasibility of an MHN can be expressed mathematically in the form of the following:

"Theorem" III.1 *Under the assumptions 1–5, for any non-empty cylinder $[\omega_0, \omega_1, \ldots, \omega_k]$ and for any neighborhood V of $\Gamma([\omega_0, \omega_1, \ldots, \omega_k])$, there exists an open set $U \subset V$ of initial points in a neighborhood of Γ_1 such that for each $x_0 \in U$, the corresponding trajectory $x(t, x_0) \in V$ for $0 \le t \le T$ and $x(T, x_0)$ belongs to a neighborhood of a saddle $Q_{l_{m_k}}^{m_k}$ labeled by the symbol ω_k, i.e., the trajectory $x(t, x_0)$ is shadowing the MHN $\Gamma([\omega_0, \omega_1, \ldots, \omega_k])$.*

We put the word Theorem in the quotation marks because we will prove this result under an additional assumption 6 although we believe that it holds without them. Assumption 6: The system (1) is C^1-linearizable in a neighborhood of each Q_i^l, $i = 1, \ldots, N$, $l = 1, \ldots, L$.

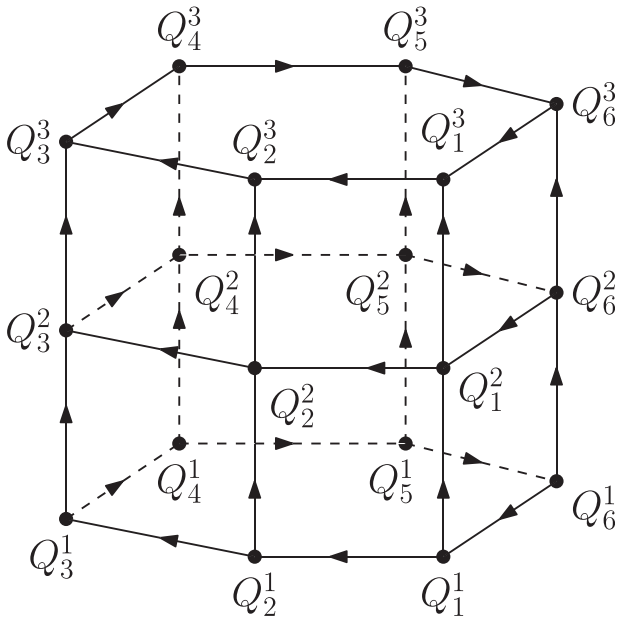

FIG. 4. An illustration of the MHN in the system when $L = 3$ and $N = 6$.

IV. REMARKS ON THEOREM

For the convenience of readers, we put the proof of Theorem III.1 into Appendix A, and here we discuss its results and main steps in the proof. In fact, this Theorem III.1 tells us that there are heteroclinic channels in a neighborhood of the heteroclinic network Γ that is labeled by non-empty cylinders (admissible words) of a topological Markov chain. We calculated the number of such channels (see Section V). It turned out that for the channels with n switchings (i.e., a representative point on a trajectory started at the beginning of such a channel meets neighborhoods of some saddle equilibrium points n times), we can estimate the number of such channels from below by a polynomial of n of degree $L-1$ (where L is the number of modalities in the system (1)). One can easily see that the number of such channels for the one-modality system is independent of n, and this is also true for direct product (uncoupled union) of such system. Thus, the main qualitative result of Theorem III.1 is that the binding of systems leads to the increase in possibilities of behaviors which is different from the "mechanical" union, i.e., binding leads to the increase in complexity of such a behavior. Also, from quantitative point of view, one can calculate this complexity function by using symbolic dynamics.

The idea of the proof can be described as follows. Given a non-empty cylinder $[\omega_0, \ldots, \omega_{n-1}]$, a sequence of saddle equilibrium points is determined, say, $Q_{\omega_0}, \ldots, Q_{\omega_{n-1}}$, where $Q_{\omega_k} \in \{Q_{l_m}^m\}$, and a sequence of heteroclinic trajectories, say, $P_{\omega_i\omega_{i+1}}, i = 0, \ldots, n-2$, is determined where $P_{\omega_i\omega_{i+1}}$ starts at Q_{ω_i} and ends at $Q_{\omega_{i+1}}$. Because of the graph G structure, each saddle Q_{ω_i} $(= Q_{l_m}^m, m \ne 1, L)$ has two heteroclinic trajectories, say, H_1^- and H_2^-, coming to it (one of them is $P_{\omega_{i-1}\omega_i}$) and two heteroclinic trajectories, say, H_1^+ and H_2^+ (one of them is $P_{\omega_i\omega_{i+1}}$) coming out of it, see Fig. 5(a). If $Q_{\omega_i} = Q_{l_m}^1$, then we deal with the only heteroclinic trajectory $P_{\omega_{i-1}\omega_i}$ joining $Q_{\omega_{i-1}} = Q_{l_m-1}^1$ and Q_{ω_i}, and two heteroclinic trajectories coming out of Q_{ω_i}. If $Q_{\omega_i} = Q_{l_m}^L$, then we deal with the only heteroclinic trajectory coming out of Q_{ω_i}, say, $P_{\omega_i\omega_{i+1}}$, where $Q_{\omega_{i+1}} = Q_{l_m+1}^L$, and two heteroclinic trajectories ending at Q_{ω_i}.

We endow each of heteroclinic trajectories with a section transversal to the flow in a neighborhood of each saddle Q_{ω_i}, H_k^- with S_k^- and H_k^+ with S_k^+, $k = 1, 2$, see Fig. 5(a). Then we show (Subsection 1 in Appendix A) that for each pair (S_k^-, S_p^+), $k, p \in \{1, 2\}$, there is an open set of initial points in a neighborhood of $H_k^- \cap S_k^-$ that is mapped by a local map along trajectories into an open set in a neighborhood of $S_p^+ \cap H_p^+$. Then this open set is moving along the

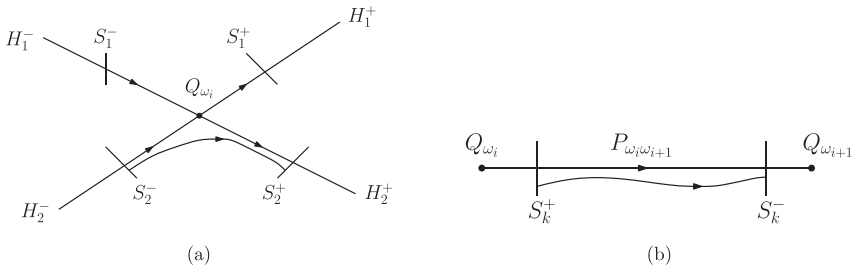

FIG. 5. Scheme of local (a) and global (b) behaviors of trajectories in a neighborhood of Γ.

heteroclinic trajectory $P_{\omega_i\omega_{i+1}}$ to a section S_k^- in a neighborhood of $Q_{\omega_{i+1}}$, Fig. 5(b). We show (see Subsection 2 in Appendix A) that this global map from $S_k^+(Q_{\omega_i})$ to $S_k^-(Q_{\omega_{i+1}})$ behaves qualitatively as a translation, thus, we can repeat our local consideration again around $Q_{\omega_{i+1}}$ and repeat the above procedures. Finally, we obtain an open set of initial points in a neighborhood of Q_{ω_0} such that the trajectory going through each of them is shadowing the MHN $\Gamma([\omega_0, \ldots, \omega_{n-1}])$.

V. SYMBOLIC COMPLEXITY OF THE SYSTEM

We have shown in Section IV that for any cylinder of the topological Markov chain (Ω_A, σ), there are trajectories of the system (1) that behave according to the symbolic description represented by the cylinder. It is natural to ask how many different itineraries the trajectories have, i.e., how many different non-empty cylinders can be realized by the system.

The symbolic complexity of the topological Markov chain (Ω_A, σ) is defined as

$$C_n = \sharp\{\text{all nonempty cylinders } [\omega_0, \omega_1, \ldots, \omega_{n-1}] \text{ of length } n\}.$$

It is known (see, for instance, page 73 in Ref. 16) that $C_n = EA^{n-1}E^T$, where $E = (1, 1, \ldots, 1)$ is the NL-row vector with all coordinates equal one and A is the transition matrix. We prove now the following lemma.

Lemma V.1 *For the topological Markov Chain (Ω_A, σ) derived by the MHN Γ, the symbolic complexity function is $C_n = P_k(n)$, where $P_k(n)$ is a polynomial of degree k and $k = L - 1$.*

To prove this lemma, we need to calculate $EA^{n-1}E^T$. It follows that the transition matrix A can be partitioned into an $L \times L$ block matrix:

$$\mathrm{A} = \begin{pmatrix} \mathrm{B} & \mathrm{I} & 0 & \ldots & 0 \\ 0 & \mathrm{B} & \mathrm{I} & 0 & \vdots \\ \vdots & \ddots & \ddots & \ddots & \vdots \\ \vdots & & \ddots & \mathrm{B} & \mathrm{I} \\ 0 & \ldots & \ldots & 0 & \mathrm{B} \end{pmatrix},$$

where I is an $N \times N$ identity matrix, $\mathbf{0}$ is an $N \times N$ zero matrix, and B is an $N \times N$ permutation matrix of the following form:

$$B = \begin{pmatrix} 0 & 1 & 0 & \ldots & 0 \\ 0 & 0 & 1 & 0 & \vdots \\ \vdots & \ddots & \ddots & \ddots & \vdots \\ 0 & \ldots & \ldots & 0 & 1 \\ 1 & 0 & \ldots & \ldots & 0 \end{pmatrix}.$$

It is easy to find that for $n \geq L$,

$$A^{n-1} = \begin{pmatrix} B^{n-1} & \binom{n-1}{1}B^{n-2} & \binom{n-1}{2}B^{n-3} & \ldots & \binom{n-1}{L-1}B^{n-L} \\ 0 & B^{n-1} & \binom{n-1}{1}B^{n-2} & \ldots & \binom{n-1}{L-2}B^{n-L+1} \\ \vdots & \ddots & \ddots & \ddots & \ddots \\ 0 & \cdots & \cdots & \cdots & B^{n-1} \end{pmatrix}. \tag{2}$$

Therefore, for $e = (1, 1, \ldots, 1)$, the N-row vector of all coordinates 1, we obtain

$$\begin{aligned} EA^{n-1}E^T &= LeB^{n-1}e^T + (L-1)\binom{n-1}{1}eB^{n-2}e^T + \cdots + 2\binom{n-1}{L-2}eB^{n-L+1}e^T + \binom{n-1}{L-1}eB^{n-L}e^T \\ &= LN + (L-1)N\binom{n-1}{1} + \cdots + 2N\binom{n-1}{L-2} + N\binom{n-1}{L-1}. \end{aligned} \tag{3}$$

Note here that an iteration of a permutation matrix is still a permutation matrix. So $eB^k e^T = N$ for any integer k when B is an $N \times N$ permutation matrix. We can see that the highest degree of n in the polynomial is determined by the term $\binom{n-1}{L-1}$. Therefore, the highest degree of n is $k = L-1$. Thus, we see here that the topological entropy

$$h = \lim_{n\to\infty} \ln C_n/n = 0.$$

This implies that the symbolic system is not chaotic. Nevertheless, the binding causes an essential changing in qualitative (and quantitative) behavior of the complexity function as it was already mentioned in Section IV.

VI. CONCLUDING REMARKS

In the framework of the our model (1), binding of different modalities means the existence in the phase space of a heteroclinic network consisting of heteroclinic cycles inside modalities subspaces and heteroclinic trajectories joining them. Because of the main theorem in the paper, there is a variety of possibilities for shadowing trajectories to stay in a neighborhood of heteroclinic cycles and to go from one cycle to another. In other words, there are many heteroclinic channels around particular paths on the graph of our network. It is a way to understand: (i) how the robustness of the binding process against a noise occurs, and (ii) how the complexity of the network increases because of the binding. Indeed, according to the point (i), one can see that small noise cannot destroy heteroclinic channel—it only can change its form a little bit. Furthermore, according to the point (ii), one can be convinced that a symbolic description is an appropriate language for the studies of complexity functions. In reality, different channels have different probabilities to be realized—the volumes of the sets of initial points corresponding to them are different. This will be the subject of further studies.

We want to emphasize that the study of heteroclinic networks and channels opens up an effective approach to understand dynamics of high dimensional models of cognitive activities and disorders. Important and interesting application of the theory presented in this paper can be used for dynamical analyses of such sequential psychiatric disorders as obsessive compulsive disorder, bipolar disorder, attention deficit, and others. Some very promising results are already in hands of psychiatrists.[17–19] As a matter of fact, behavior, perception, and cognition are strongly shaped by the synthesis of time dependent information across the different sensory modalities. This is the binding dynamics. Such multisensory integration often results in performance and perceptual benefits that reflect the effective information conferred by having cues from multiple sequential modalities, such as in the process of perception of speech—auditory and visual.[20] The time interval during which information from different modalities is dynamically integrated is called the temporal binding window.[21] Emerging evidence suggests that such temporal window is altered in a series of disorders, including autism, dyslexia, and schizophrenia.[21] Keeping in mind that the stability of the binding window and dynamical capacity of the binding process depend on the value of control parameters in the binding model, it looks very perspective to connect these parameters with plasticity within relevant sensory modalities.[22] Similar problems are important for other cognitive processes, in particular, for working memory[23] and attention.[24]

ACKNOWLEDGMENTS

The authors thank T. Young for useful suggestions. V.A. was partially supported by the Federal Target Program of the Russian Ministry of Education and Science, Grant No. 14.584.21.0010, ID RFMEFI58414X0010.

APPENDIX A: PROOF OF THE THEOREM

Because of the form of the system (1), one can easily see that the matrix of the linearization of system (1) at Q_i^l can be diagonalized even in the case where some of its eigenvalues are of multiplicity greater than 1. We denote by y_1, y_2 the variables corresponding to the eigenvectors related to the positive eigenvalues and by x_i those related to the negative ones. Thus, under the assumptions 1–6, the system (1) in a neighborhood of Q_i^l can be rewritten as

$$\begin{aligned} \dot{y}_1 &= \gamma_1 y_1, \\ \dot{y}_2 &= \gamma_2 y_2, \\ \dot{\mathbf{x}} &= A\mathbf{x}, \end{aligned} \tag{A1}$$

where $0 < \gamma_1 = \lambda^l_{ii+1}$ and $0 < \gamma_2 = \lambda^l_{iN+l+1}$, so $0 < \gamma_2 < \gamma_1$ according to assumptions 1, 4, and 5. In Eq. (A1), $\mathbf{x} = (x_1, \ldots, x_m) \in \mathbb{R}^m$, where $m = L(N-2)$, and

$$||e^{At}|| \le e^{\mu t}, \quad \mu < 0, \quad t \ge 0. \tag{A2}$$

Let us remark that here, in the proof of the Theorem, we use the same letter "x" as in (1). We hope it will not confuse a reader.

Without loss of generality, we assume that x_1 is the coordinate corresponding to the leading direction of the intersection of the stable manifold of Q_i^l with the plane $\{x_j^m = 0, m \ne l\}$ (see the assumption 2). The coordinate x_2 corresponds to the eigenvector related to the eigenvalue $\sigma_i^{l-1} - \sigma_i^l \xi_{ii}^{l-1l} < 0$, i.e., it corresponds to the direction of the heteroclinic trajectory joining the equilibrium points Q_i^{l-1} and Q_i^l under which it comes to Q_i^l.

The intersections of a neighborhood of Q_i^l with the heteroclinic trajectories belonging to the MHN starting at Q_i^l have the equations

$$\mathbf{x} = 0, \quad y_2 = 0$$

for a local piece of the trajectory in the heteroclinic cycle Γ_l, and

$$\mathbf{x} = 0, \quad y_1 = 0$$

for a piece of the trajectory joining Q_i^l and Q_i^{l+1}. Furthermore, the local pieces of the heteroclinic trajectories ending at Q_i^l have the equations

$$y_1 = y_2 = 0, x_j = 0, \text{ where } j \neq 1$$

for the trajectory in the heteroclinic cycle Γ_l and

$$y_1 = y_2 = 0, x_j = 0, \text{ where } j \neq 2$$

for the trajectory joining Q_i^{l-1} and Q_i^l.

To prove the Theorem, i.e., to find trajectories that shadow the MHN, we endow the MHN with a sequence of sections transversal to the flow and we will study images (and preimages) of regions on these sections with respect to the corresponding maps. Thus, we introduce

$$S_1^- = \{(\mathbf{x},\mathbf{y}) : x_1 = \delta, |(x_2,\ldots,x_m)| \le \varepsilon, |y_1| \le \varepsilon, |y_2| \le \varepsilon\},$$
$$S_2^- = \{(\mathbf{x},\mathbf{y}) : x_2 = \delta, |(x_1,x_3,\ldots,x_m)| \le \varepsilon, |y_1| \le \varepsilon, |y_2| \le \varepsilon\},$$
$$S_1^+ = \{(\mathbf{x},\mathbf{y}) : y_1 = \delta, |y_2| \le \varepsilon, |\mathbf{x}| \le \varepsilon\},$$
$$S_2^+ = \{(\mathbf{x},\mathbf{y}) : y_2 = \delta, |y_1| \le \varepsilon, |\mathbf{x}| \le \varepsilon\},$$

where ε is a small parameter which is, in fact, the size (diameter) of the section. Remark that all the variables are supposed to be non-negative. Moreover, we will write $S_{1,2}^-(Q_i^l)$, $S_{1,2}^+(Q_i^l)$ where it will be necessary.

1. Local maps

To construct a map $T_{i1} : S_i^- \to S_1^+$, $i = 1, 2$, we solve the system (A1) to obtain that

$$y_1(t) = y_{10}e^{\gamma_1 t},$$
$$y_2(t) = y_{20}e^{\gamma_2 t},$$
$$\mathbf{x}(t) = \mathbf{x}_0 e^{At},$$

where $(y_{10}, y_{20}, \mathbf{x}_0) \in S_i^-$ is the initial condition. We can find the transition time t_1 from the restriction that $y_1(t_1) = \delta$:

$$t_1 = 1/\gamma_1 \ln(\delta/y_{10}).$$

So, we can write the formulas for T_{i1}:

$$y_2(t_1) = y_{20}(\delta/y_{10})^{\gamma_2/\gamma_1},$$
$$\mathbf{x}(t_1) = \mathbf{x}_0 e^{At_1}.$$

We need to prove the claim that $y_2(t_1) \le \varepsilon$, which is equivalent to

$$y_{20} \le \delta^{-\gamma_2/\gamma_1}\varepsilon(y_{10})^{\gamma_2/\gamma_1}. \tag{A3}$$

If $y_{10} = \varepsilon$, the right hand side of (A3) is $\delta^{-\gamma_1/\gamma_2}\varepsilon^{1+\gamma_2/\gamma_1}$, which is less than ε if $\varepsilon \ll 1$. So the projection of the domain of T_{i1} onto the y-plane looks as D_1 in Fig. 6.

To construct $T_{i2} : S_i^- \to S_2^+$, similarly, we find the transition time

$$t_2 = 1/\gamma_2 \ln(\delta/y_{20}),$$

and obtain

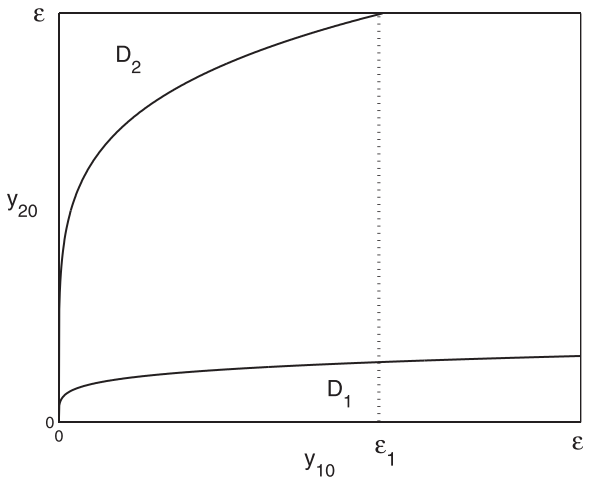

FIG. 6. The projection of the domain of T_{i1} and T_{i2} onto the y-plane.

$$y_1(t_2) = y_{10}(\delta/y_{20})^{\gamma_1/\gamma_2}.$$

The condition $y_1(t_2) \le \varepsilon$ implies the inequality

$$y_{20} \ge \delta\varepsilon^{-\gamma_2/\gamma_1}(y_{10})^{\gamma_2/\gamma_1}, \tag{A4}$$

so the projection of the domain of T_2 onto the y-plane looks as region D_2 in Fig. 6 where

$$\varepsilon_1 = \delta^{-\gamma_1/\gamma_2}\varepsilon^{1+\gamma_1/\gamma_2} \le \varepsilon \quad \text{if} \quad \varepsilon \ll 1,$$

provided that $\delta\varepsilon^{-\gamma_2/\gamma_1} > \delta^{-\gamma_2/\gamma_1}\varepsilon$, which is true if $\varepsilon \ll 1$. Let us remark that Fig. 6 is the same for $i = 1$ or 2.

Denote by $\mathrm{dom}T_{ij}$ the domain of T_{ij}, $i,j \in \{1, 2\}$. We show now that T_{i1} ($\mathrm{dom}T_{i1}$) contains, for small values of ε, the rectangle $R_\alpha^1 = \{(\mathbf{x}, y_2) | \, |\mathbf{x}| \le \alpha, 0 < y_2 \le \varepsilon\}$ and T_{i2} ($\mathrm{dom}T_{i2}$) contains the rectangle $R_\alpha^2 = \{(\mathbf{x}, y_1) | \, |\mathbf{x}| \le \alpha, x_1 > 0, 0 < y_1 \le \varepsilon\}$. Consider, for instance, T_{12}. We have

$$x_1 = \delta e^{\lambda_1 t_2} = \delta(\delta/y_{20})^{\lambda_2/\gamma_1},$$

so

$$y_{20} = \delta^{\gamma_1/\lambda_2+1}x_1^{-\gamma_1/\lambda_2}.$$

We claim that $y_{20} \le \varepsilon$, therefore,

$$0 < x_1 \le \varepsilon^{-\lambda_1/\gamma_1}\delta^{1+\lambda_2/\gamma_1} =: \alpha_1.$$

We already know that for D_2, $y_1 = y_1(t_2) \le \varepsilon$. Now for $k \neq 1$,

$$x_\alpha = x_{k0}e^{\lambda_k t_2} = x_{k0}\delta^{\lambda_k/\gamma_1}y_{20}^{-\lambda_k/\gamma_1},$$

so

$$\max|x_k| = \varepsilon\delta^{\lambda_k/\gamma_1}\varepsilon^{-\lambda_k/\gamma_1} =: \alpha_k.$$

Thus, every point $(\mathbf{x}, y_1)$ where $0 < x_1 \le \alpha_1, |x_1| \le \alpha_k, 0 \le y_1 \le \varepsilon$ is the image of a point on S_1^- under the map T_{12}. Defining α as $\min\alpha_k$, we obtain the desired result. The proof is the same for other mappings T_{ij}.

2. Global maps

We define the global map along the trajectories close to the heteroclinic orbit joining Q_i^l and Q_{i+1}^l as

$$T_1^{gl} : S_1^+(Q_i^l) \to S_1^-(Q_{i+1}^l).$$

This is a diffeomorphism and it is well-defined because of the finite transition time from a neighborhood of Q_i^l to a neighborhood of Q_{i+1}^l along the corresponding heteroclinic orbit. Similarly, the global map (a diffeomorphism) along the trajectories close to the heteroclinic one joining Q_i^l and Q_i^{l+1} is well-defined as well. It is denoted as

$$T_2^{gl} : S_2^+(Q_i^l) \to S_2^-(Q_i^{l+1}).$$

To write the formulas for the global maps in the $(\mathbf{x}, \mathbf{y})$-coordinates, one needs to use formulas for the sections $S_{1,2}^+(Q_i^l), S_{1,2}^-(Q_{i+1}^l)$, and $S_{1,2}^-(Q_i^{l+1})$ in the original coordinates $\{x_i^l\}$, to integrate the system (1) over finite transition time, and to present the images in the new $(\mathbf{x}, \mathbf{y})$-coordinates. But we do not need them—we use only the claim that these $(\mathbf{x}, \mathbf{y})$-formulas determine diffeomorphisms, that follows easily from the facts that changes of variables we used are diffeomorphisms and the global maps in the $\{x_i^l\}$-coordinates are also diffeomorphisms. The main fact to be checked is that the points with non-negative values of the $\mathbf{y}$-coordinates are mapped into those with the same property. This is true. Indeed,

(i) For the system (1), the positive (non-negative) "octant" is an invariant set that can be checked directly.
(ii) Each (x_α, x_β)-plane where $x_\alpha = x_{i_1}^{l_1}, x_\beta = x_{i_2}^{l_2}$ and i_1, i_2, l_1, l_2 are arbitrary indices, is invariant.
(iii) A piece of the phase portrait on the (x_i^l, x_{i+1}^l)-plane (or on the (x_i^l, x_i^{l+1})-plane) looks as in the Fig. 7 (see Table I for the eigenvectors).

The similar picture is observed on the (x_i^l, x_i^{l+1})-plane. It implies that the maps T_1^{gl} and T_2^{gl} send points with non-negative values of the $\mathbf{y}$-coordinates in a neighborhood of Q_i^l into those with non-negative values of the $\mathbf{y}$-coordinates in neighborhoods of Q_{i+1}^l and Q_i^{l+1} correspondingly. The same is true for the values of the x_k coordinates where $k = 1, 2$.

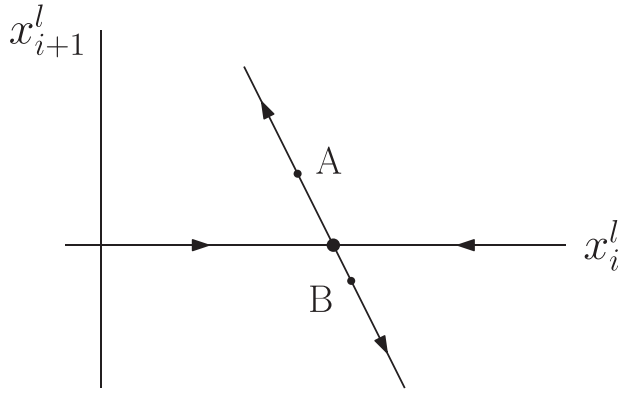

FIG. 7. Positive values of y_1 (point A) correspond to the positive values of x_{i+1}^l. The negative values (point B) correspond to the negative ones.

Hence, the sets

$$R_\alpha^1 \cap (T_1^{gl})^{-1}(S_1^-(Q_{i+1}^l)) \subset S_1^+(Q_i^l) \quad \text{and}$$
$$R_\alpha^2 \cap (T_2^{gl})^{-1}(S_2^-(Q_i^{l+1})) \subset S_2^+(Q_i^l)$$

contain non-empty interiors.

3. Images and preimages

It follows now that the projection onto the $\mathbf{y}$-plane of the set

$$(T_1)^{-1}((T_1^{gl})^{-1}(S_1^-(Q_{i+1}^l)) \cap R_\alpha^1)$$

belongs to D_1, no matter whether $S^-(Q_i^l) = S_1^-(Q_i^l)$ or $S^-(Q_i^l) = S_2^-(Q_i^l)$. We let this projection to be denoted as $\tilde{D}_1$. Similarly, the projection of the set

$$(T_2)^{-1}((T_2^{gl})^{-1}(S_2^-(Q_i^{l+1})) \cap R_\alpha^2)$$

onto the $\mathbf{y}$-plane, say, $\tilde{D}_2$, belongs to D_2. Therefore, a trajectory going through an initial point $(\mathbf{x}_0, \mathbf{y}_0)$ on $S_i^-(Q_i^l)$, $i = 1, 2$, with small values of the $\mathbf{x}_0$-coordinates and $\mathbf{y}_0 \in \tilde{D}_1$ will intersect $S_1^+(Q_i^l)$ and then will follow the heteroclinic trajectory joining Q_i^l and Q_{i+1}^l, up to the intersection with $S_1^-(Q_{i+1}^l)$.

Similarly, the trajectory going through $(\mathbf{x}_0, \mathbf{y}_0)$ and where $\mathbf{y}_0 \in \tilde{D}_2$ and small $|\mathbf{x}_0|$ will intersect $S_2^+(Q_i^l)$ and will shadow the heteroclinic orbit joining Q_i^l and Q_i^{l+1} up to the intersection with $S_2^-(Q_i^{l+1})$.

The same consideration can be performed in a neighborhood of Q_{i+1}^l and Q_i^{l+1}. For instance, for Q_{i+1}^l, we again have four local maps

$$T_{ij} : S_i^-(Q_{i+1}^l) \to S_j^+(Q_{i+1}^l), \text{ where } i, j = 1, 2.$$

Projections of $\mathrm{dom}T_{ij}$ onto the $\mathbf{y}$-plane look exactly as D_1 and D_2 in Fig. 6. Moreover, since $\mathrm{dom}T_{1j} \subset S_1^-(Q_{i+1}^l)$, the map $(T_1^{gl})^{-1}$ is well-defined on it. Thus on $S_1^-(Q_i^l)$, we have two regions $(T_{11})^{-1}((T_1^{gl})^{-1}\mathrm{dom}T_{11} \cap R_\alpha^1)$ and $(T_{12})^{-1}((T_1^{gl})^{-1}\mathrm{dom}T_{12} \cap R_\alpha^2)$. Denote by D_{11} and D_{12} their projections onto the $\mathbf{y}$-plane. They look as in Fig. 8.

We can obtain then the regions $(T_{22})^{-1}((T_2^{gl})^{-1}(\mathrm{dom}T_{2j}) \cap R_\alpha^2))$ on $S_2^-(Q_i^l)$ and their projections D_{2j} onto the $\mathbf{y}$-plane, with $j = 1, 2$. Similarly, we can also obtain the regions $(T_{12})^{-1}((T_2^{gl})^{-1}\mathrm{dom}T_{2j} \cap R_\alpha^2), j = 1, 2$ on $S_1^-(Q_i^l)$ and $(T_{21})^{-1}((T_1^{gl})^{-1}\mathrm{dom}T_{1j} \cap R_\alpha^1), j = 1, 2$ on $S_2^-(Q_i^l)$. Their projections onto the y-plane are denoted as $\tilde{D}_{ij}$, which look similarly as $D_{i,j}$.

Therefore, if $(\mathbf{x}_0, \mathbf{y}_0)$ on $S_1^-(Q_i^l) \cup S_2^-(Q_i^l)$ has small $|\mathbf{x}_0|$ and $\mathbf{y}_0 \in D_{\alpha\beta} \cup \tilde{D}_{\alpha\beta}$, then the corresponding trajectory intersects $S_\alpha^+(Q_i^l)$ first, then follows the corresponding heteroclinic trajectory and intersects $S_{1,2}^-(Q_{i+1}^l)$ if $\alpha = 1$ or $S_{1,2}^-(Q_i^{l+1})$ if $\alpha = 2$. After this, the trajectory comes to a neighborhood of the heteroclinic orbit joining: (i) Q_{i+1}^l and Q_{i+2}^l if $\alpha = \beta = 1$, (ii) Q_{i+1}^l and Q_{i+1}^{l+1} if $\alpha = 1$ and $\beta = 2$, (iii) Q_i^{l+1} and Q_{i+1}^{l+1} if $\alpha = 2$ and $\beta = 1$, and (iv) Q_i^{l+1} and Q_i^{l+2} if $\alpha = \beta = 2$.

Since these initial points contain open sets, we in fact proved the Theorem for cylinders $[\omega_0, \omega_1, \omega_2]$, where ω_0 corresponds to Q_i^l, and ω_1, ω_2 correspond to $Q_{i+1}^l, Q_i^{l+1}, Q_{i+2}^l$, and Q_i^{l+2}.

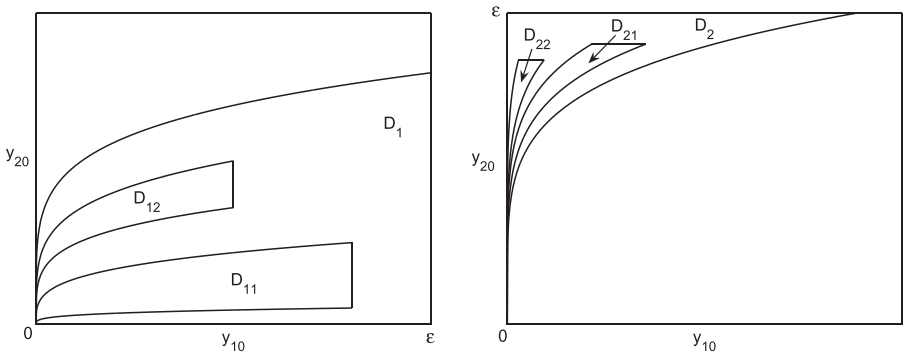

FIG. 8. Projections onto the y-plane of preimages of compositions of local and global maps.

Exactly in the same way, one can prove the Theorem for an arbitrary cylinder $[\omega_0, \omega_1,\ldots,\omega_k]$.

APPENDIX B: WINNERLESS COMPETITION AND HETEROCLINIC CHANNELS IN SYSTEM WITH INHIBITION: HISTORICAL VIEW

1. Autonomous competitive dynamics

The classical Gause-Lotka-Volterra model for N competitors in the generalized form is

$$\frac{d}{dt}R_i = R_i\Big[\mu_i(S) - \Sigma_{j=1}^{N}\rho_{ij}R_j + \eta(t)\Big].$$

When the matrix elements and parameter S are constants, and noise is absent, we name the model *canonical*. The system dynamics critically depends on the number and features of the metastable states. A metastable state temporarily holds stationary values. It is characterized by a slowing down of the system motion in a vicinity of the stationary state. In the graph of N-observable competitors, this phenomenon is

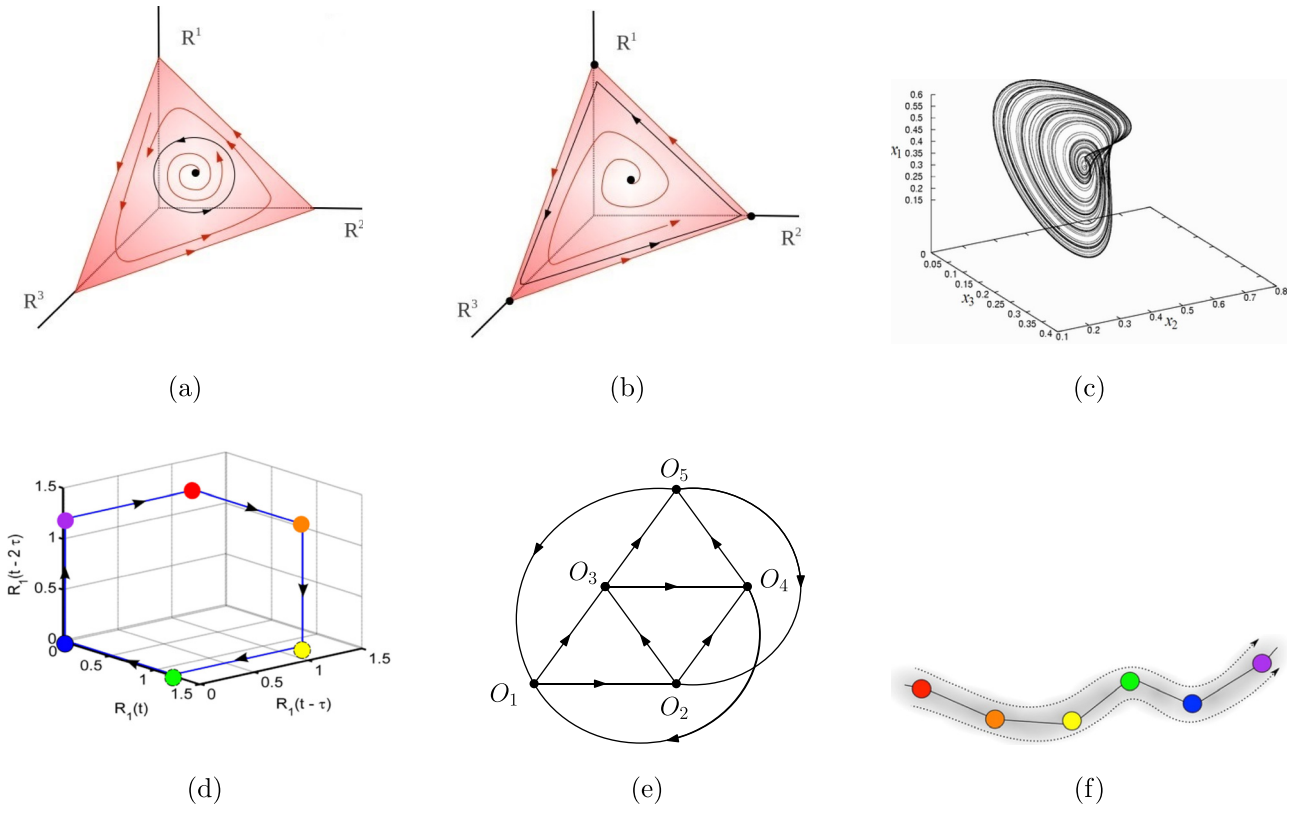

FIG. 9. Stable limit cycle (panel (a)) and heteroclinic cycle (panel (b)) on 2-D simplex (canonical model with $N=3$), see Refs. 25–28. Figures are reprinted from M. Rabinovich, I. Tristan, and P. Varona, "Neural dynamics of attentional cross-modality control," PLoS ONE **8**, e64406 (2013).[29] Many others describe stable oscillations in competitive ensembles. For example, see Ref. 30 for an interesting piecewise linear model. Panel (c) shows that in some area of control parameters of the canonical model with $N=4$, a strange attractor exists. One can see that a 3-D projection of the attractor looks like Rössler's folded band attractor.[31] Reprinted with permission from J. Vano, J. Wildenburg, M. Anderson, J. Noel, and J. Sprott, "Chaos in low-dimensional Lotka-Volterra models of competition," Nonlinearity **19**, 2391 (2006). Copyright 2006 IOP Publishing. Panel (d) shows the stable heteroclinic cycle in the canonic model with $N=6$. Each saddle has one-dimensional unstable separatrix that forms a heteroclinic contour.[7] Panel (e) shows that for $N=5$ in the phase space of the canonical model, there exists a two-dimensional heteroclinic attractor that includes saddles O_j with two unstable separatrices.[32] Panel (f) shows the robust heteroclinic channel—a vicinity of a six-saddle chain, the saddle value of each saddle is larger than one.[7] Figures (d) and (f) are reprinted from M. Rabinovich, Y. Sokolov, and R. Kozma, "Robust sequential working memory recall in heterogeneous cognitive networks," Front. Syst. Neurosci. **8**, 220 (2014).[33]

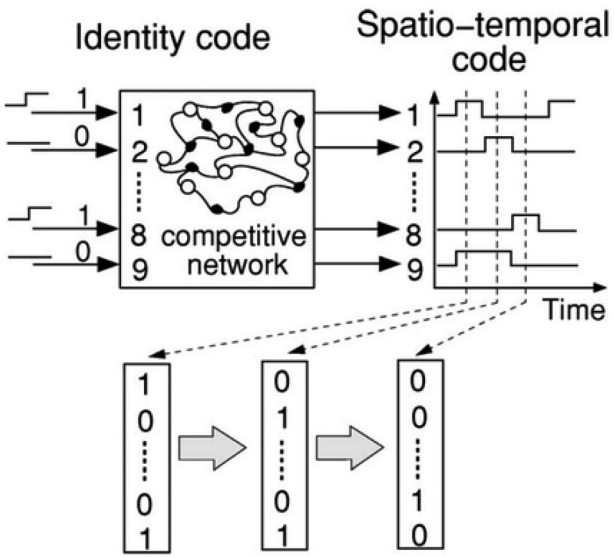

FIG. 10. Dynamical coding—input dependent WLC.[4,34] Reprinted with permission from M. I. Rabinovich, P. Varona, A. I. Selverston, and H. D. Abarbanel, "Dynamical principles in neuroscience," Rev. Mod. Phys. **78**, 1213 (2006). Copyright 2006 The American Physical Society.

represented by a plateau or pause. The image of a metastable state in the phase space is a saddle point. Fig. 9 summarizes some of the previous works on this canonical model.

Note that a SHC is formed by a sequence of saddle states, heteroclinic trajectories, and their vicinity. If the compressing of the phase volume around the SHC is stronger than the stretching of the volume along the SHC, the trajectories that are attracted by the SHC cannot leave it until the last equilibrium point. SHC is an image of robust transient behavior in a dynamical system.

From these previous work, one can see that for $N > 3$, the canonical model can have, in the phase space, a heteroclinic network with more complex topology than the heteroclinic contour formed by one dimensional unstable separatrices. It can be a 2-D heteroclinic attractor or the interaction of several heteroclinic contours that forms a joint network, like a binding process.

2. Non-autonomous competitive dynamics

WLC: A general dynamical phenomenon that causes sequential switching of prevalence among participants. For example, if in a head-to-head competition, boxer A beats boxer B, boxer B beats boxer C, and finally boxer C beats boxer A, all participants are "winners" for a finite time, but there is no overall winner, such as in "winner takes all." A basic model with the connection matrix elements depending on stimuli is very convenient for dynamical analyses and prediction of cognitive processes.[5,15] Fig. 10 shows the transformation of the identity spatial input into spatiotemporal output based on the intrinsic sequential dynamics of a neural ensemble with WLC.

[1]B. C. Dickerson and H. Eichenbaum, "The episodic memory system: Neurocircuitry and disorders," Neuropsychopharmacology **35**, 86–104 (2010).
[2]V. A. Diwadkar, P. A. Carpenter, and M. A. Just, "Collaborative activity between parietal and dorso-lateral prefrontal cortex in dynamic spatial working memory revealed by fMRI," Neuroimage **12**, 85–99 (2000).
[3]K. Nashiro and M. Mather, "The effect of emotional arousal on memory binding in normal aging and Alzheimer's disease," Am. J. Psychol. **124**, 301–312 (2011).
[4]M. Rabinovich, A. Volkovskii, P. Lecanda, R. Huerta, H. Abarbanel, and G. Laurent, "Dynamical encoding by networks of competing neuron groups: Winnerless competition," Phys. Rev. Lett. **87**, 068102 (2001).
[5]M. I. Rabinovich, R. Huerta, P. Varona, and V. S. Afraimovich, "Transient cognitive dynamics, metastability, and decision making," PLoS Comput. Biol. **4**, e1000072 (2008).
[6]M. I. Rabinovich, K. J. Friston, and P. Varona, *Principles of Brain Dynamics: Global State Interactions* (MIT Press, 2012).
[7]C. Bick and M. I. Rabinovich, "Dynamical origin of the effective storage capacity in the brain's working memory," Phys. Rev. Lett. **103**, 218101 (2009).
[8]K. Friston, C. Frith, and R. Frackowiak, "Principal component analysis learning algorithms: A neurobiological analysis," Proc. R. Soc. London, Ser. B **254**, 47–54 (1993).
[9]J. Kelso, A. Fuchs, R. Lancaster, T. Holroyd, D. Cheyne, and H. Weinberg, "Dynamic cortical activity in the human brain reveals motor equivalence," Nature **392**, 814–818 (1998).
[10]A. McIntosh, F. Bookstein, J. V. Haxby, and C. Grady, "Spatial pattern analysis of functional brain images using partial least squares," Neuroimage **3**, 143–157 (1996).
[11]A. J. Bell and T. J. Sejnowski, "An information-maximization approach to blind separation and blind deconvolution," Neural Comput. **7**, 1129–1159 (1995).
[12]S. Makeig, T. P. Jung, A. J. Bell, D. Ghahremani, and T. J. Sejnowski, "Blind separation of auditory event-related brain responses into independent components," Proc. Natl. Acad. Sci. **94**, 10979–10984 (1997).
[13]A. Banerjee, A. S. Pillai, and B. Horwitz, "Using large-scale neural models to interpret connectivity measures of cortico-cortical dynamics at millisecond temporal resolution," Front. Syst. Neurosci. **5**, 102 (2011).
[14]M. I. Rabinovich, V. S. Afraimovich, and P. Varona, "Heteroclinic binding," Dyn. Syst. **25**, 433–442 (2010).
[15]M. I. Rabinovich, A. N. Simmons, and P. Varona, "Dynamical bridge between brain and mind," Trends Cognit. Sci. **19**, 453–461 (2015).
[16]V. Afraimovich and S. Hsu, *Lectures on Chaotic Dynamical Systems* (American Mathematical Society Providence, 2003).
[17]A. Bystritsky, A. Nierenberg, J. Feusner, and M. Rabinovich, "Computational non-linear dynamical psychiatry: A new methodological paradigm for diagnosis and course of illness," J. Psychiatr. Res. **46**, 428–435 (2012).
[18]G. Schiepek, I. Tominschek, S. Heinzel, M. Aigner, M. Dold, A. Unger, G. Lenz, C. Windischberger, E. Moser, M. Plöderl *et al.*, "Discontinuous patterns of brain activation in the psychotherapy process of obsessive compulsive disorder: Converging results from repeated FMRI and daily self-reports," PloS One **8**, e71863 (2013).
[19]A. M. Hayes, C. Yasinski, J. B. Barnes, and C. L. Bockting, "Network destabilization and transition in depression: New methods for studying the dynamics of therapeutic change," Clin. Psychol. Rev. (2015).
[20]R. A. Stevenson, M. Segers, S. Ferber, M. D. Barense, and M. T. Wallace, "The impact of multisensory integration deficits on speech perception in children with autism spectrum disorders," Front. Psychol. **5**, 379 (2014).
[21]M. T. Wallace and R. A. Stevenson, "The construct of the multisensory temporal binding window and its dysregulation in developmental disabilities," Neuropsychologia **64**, 105–123 (2014).
[22]A. R. Powers, A. R. Hillock, and M. T. Wallace, "Perceptual training narrows the temporal window of multisensory binding," J. Neurosci. **29**, 12265–12274 (2009).
[23]M. Quak, R. E. London, and D. Talsma, "A multisensory perspective of working memory," Front. Human Neurosci. **9**, 197 (2015).
[24]D. Talsma, "Predictive coding and multisensory integration: An attentional account of the multisensory mind," Front. Integr. Neurosci. **9**, 19 (2015).
[25]R. M. May and W. J. Leonard, "Nonlinear aspects of competition between three species," SIAM J. Appl. Math. **29**, 243–253 (1975).
[26]D. F. Toupo and S. H. Strogatz, "Nonlinear dynamics of the rock-paper-scissors game with mutations," Phys. Rev. E **91**, 052907 (2015).
[27]M. E. Gilpin, "Limit cycles in competition communities," Am. Nat. **109**, 51–60 (1975).
[28]J. Hofbauer and J.-H. So, "Multiple limit cycles for three dimensional Lotka-Volterra equations," Appl. Math. Lett. **7**, 65–70 (1994).
[29]M. Rabinovich, I. Tristan, and P. Varona, "Neural dynamics of attentional cross-modality control," PLoS ONE **8**, e64406 (2013).

[30]L. Glass and J. S. Pasternack, "Prediction of limit cycles in mathematical models of biological oscillations," Bull. Math. Biol. **40**, 27–44 (1978).
[31]J. Vano, J. Wildenberg, M. Anderson, J. Noel, and J. Sprott, "Chaos in low-dimensional Lotka-Volterra models of competition," Nonlinearity **19**, 2391 (2006).
[32]V. Afraimovich, G. Moses, and T. Young, "Two dimensional heteroclinic attractor in the generalized Lotka-Volterra system," Nonlinearity (submitted), arXiv:1509.04570 [math.DS]; available at http://arxiv.org/abs/1509.04570.
[33]M. I. Rabinovich, Y. Sokolov, and R. Kozma, "Robust sequential working memory recall in heterogeneous cognitive networks," Front. Syst. Neurosci. **8**, 220 (2014).
[34]M. I. Rabinovich, P. Varona, A. I. Selverston, and H. D. Abarbanel, "Dynamical principles in neuroscience," Rev. Mod. Phys. **78**, 1213 (2006).
[35]O. Kolodny and S. Edelman, "The problem of multimodal concurrent serial order in behavior," Neuroscience & Biobehavioral Reviews **56**, 252–265 (2015).